



Article

Spectroscopic Measurement of Hydrogen Atom Density in a Plasma Produced with 28 GHz ECH in QUEST

Satoru Mori ^{1,*}, Taiichi Shikama ^{1,*} , Kazuaki Hanada ², Nao Yoneda ¹, Arseniy Kuzmin ¹ , Masahiro Hasuo ¹, Hiroshi Idei ², Takumi Onchi ², Akira Ejiri ³, Yuki Osawa ³, Yi Peng ³, Kyohei Matsuzaki ³, Shinichiro Kado ⁴, Keiji Sawada ⁵, Takeshi Ido ², Kazuo Nakamura ², Ryuya Ikezoe ², Yoshihiko Nagashima ², Makoto Hasegawa ², Kengo Kuroda ², Aki Higashijima ², Takahiro Nagata ² and Shun Shimabukuro ²

¹ Department of Mechanical Engineering and Science, Graduate School of Engineering, Kyoto University, Kyoto 615-8540, Japan; yoneda.nao.45m@st.kyoto-u.ac.jp (N.Y.); kuzmin.arseniy.6x@kyoto-u.ac.jp (A.K.); hasuo@kues.kyoto-u.ac.jp (M.H.)

² Research Institute for Applied Mechanics, Kyushu University, Fukuoka 816-8580, Japan; hanada@triam.kyushu-u.ac.jp (K.H.); idei@triam.kyushu-u.ac.jp (H.I.); onchi@triam.kyushu-u.ac.jp (T.O.); t.ido@triam.kyushu-u.ac.jp (T.I.); nakamura@triam.kyushu-u.ac.jp (K.N.); ikezoe@triam.kyushu-u.ac.jp (R.I.); nagashima@triam.kyushu-u.ac.jp (Y.N.); hasegawa@triam.kyushu-u.ac.jp (M.H.); kuroda@triam.kyushu-u.ac.jp (K.K.); higashi@triam.kyushu-u.ac.jp (A.H.); nagata@triam.kyushu-u.ac.jp (T.N.); shimabukuro@triam.kyushu-u.ac.jp (S.S.)

³ Graduate School of Frontier Sciences, The University of Tokyo, Chiba 277-8561, Japan; ejiri@edu.k.u-tokyo.ac.jp (A.E.); osawa@fusion.k.u-tokyo.ac.jp (Y.O.); peng@fusion.k.u-tokyo.ac.jp (Y.P.); kasukanakaori2456@ezweb.ne.jp (K.M.)

⁴ Institute of Advanced Energy, Kyoto University, Kyoto 610-0011, Japan; kado@iae.kyoto-u.ac.jp

⁵ Graduate School of Engineering, Shinshu University, Nagano 380-8553, Japan; ksawada@shinshu-u.ac.jp

* Correspondence: satoru.mori.0731@gmail.com (S.M.); shikama@me.kyoto-u.ac.jp (T.S.)

Received: 23 June 2020; Accepted: 31 July 2020; Published: 18 August 2020



Abstract: The spatial distribution of the hydrogen atom density was evaluated in a spherical tokamak (ST) plasma sustained only with 28 GHz electron cyclotron heating (ECH). The radially resolved H_{δ} emissivity was measured using multiple viewing chord spectroscopy and Abel inversion. A collisional-radiative (CR) model analysis of the emissivity resulted in a ground-state hydrogen atom density of 10^{15} – 10^{16} m^{−3} and an ionization degree of 1–0.85 in the plasma.

Keywords: spherical tokamak; QUEST; ECH; spectroscopy; neutral; atom; ionization degree

1. Introduction

Q-shu University Experiment with Steady-State Spherical Tokamak (QUEST) is a medium-sized spherical tokamak (ST) device operated for the understanding of plasma–wall interactions in steady-state discharges [1] and for the development of non-inductive ST start-up schemes [2,3]. This study contributes to the latter by investigating the effect of neutrals (atoms) on an initial plasma produced with electron cyclotron heating (ECH).

In the ST discharge produced with ECH, a cylindrical plasma in an open field equilibrium is initially produced around the resonance layer [2,4,5]. Then, by ramping up the plasma current, an ST plasma sustained only with ECH is formed [2,4,6]. Among the characteristics of the initial ST plasma is a large variation in ion toroidal velocity in the range of 0–20 km/s with the size and position of the last closed flux surface (LCFS) [7]. Since this characteristic could be used for the active control of the flow profile, we intended to further investigate the driving and damping mechanisms of the flow. In this

study, we measured the radial distribution of the atom density and the degree of ionization (DOI) in order to evaluate the loss and transport of the ion momentum through the charge-exchange reaction (e.g., [8]), since the bulk electron temperature and density of the initial plasmas are typically less than 1 keV and $1 \times 10^{19} \text{ m}^{-3}$ [2,6,9], respectively, and these relatively small plasma parameters can result in a greater effect of atoms.

2. Experimental Setup

We performed experiments using a discharge sustained only with 28 GHz ECH. This discharge is described in detail elsewhere [2]. Briefly, the plasma was mainly heated by second harmonic resonance ECH at $R = 0.32 \text{ m}$ with a power of 120 kW, where R is the major radius. We used two discharges performed with an identical setup, i.e., one for Thomson scattering (#41176) and the other for spectroscopy (#41178) measurements. The reproducibility of plasma parameters for these discharges is within their uncertainties. Figure 1a shows the temporal evolutions of the plasma current, electron temperature T_e , and density n_e at the core [9], and the chord-integrated H_α intensity measured on a radial viewing chord on the midplane. We conducted all the measurements in the time period $t = 2.7\text{--}3.0 \text{ s}$ denoted by the shaded area in Figure 1a. The period was in the flattop phase, where the magnetic field coil currents were kept constant. The reconstructed equilibrium magnetic flux surfaces are shown in Figure 1b; these surfaces were obtained from the measured magnetic flux and plasma current using a modification of the method described in [10]. The plasma minor radius was reduced to approximately 0.1 m to increase the volume power density of the heating. The magnetic axis was located at $R = 0.32 \text{ m}$ and $z = -0.1 \text{ m}$, and the last closed flux surface (LCFS) was located at $R = 0.25$ and 0.4 m on the midplane.

Figure 2 is a schematic illustration of the visible spectroscopic system. We measured the H_δ emission line spectrum ($p = 2\text{--}6$), where p is the principal quantum number, using 24 fan-shaped viewing chords on the midplane. The distance between the viewing chord and the torus axis, which we define as η , ranged between 0.24 and 1.01 m. The diameters of the viewing spots were approximately 30 mm at the positions closest to the torus axis.

The emission was collected using two sets of a collimator (Edmund Optics Japan, Japan, TS achromatic lens; 15 mm focal length, $\phi 14 \text{ mm}$) and an optical fiber bundle (Mitsubishi Cable Industries, Japan, STU230D; 230 and 250 μm core and cladding diameters, respectively, 0.2 NA). The collected emission was transferred to a Czerny–Turner spectrometer (Acton Research, USA, AM-510; 1 m focal length, F/8.7, 1800 grooves/mm grating) equipped with astigmatism compensation optics. The spectra were recorded with a CCD (Andor Technology, UK, DU440-BU2; 2048×512 pixels, 13.5 μm pixel size, 16 bit). We set the entrance slit width of the spectrometer at 50 μm and the central output wavelength at 412 nm. The instrumental width at the full width at half maximum and the reciprocal linear dispersion were 40 pm and 6.5 pm/pixel, respectively. The sensitivity of the system was absolutely calibrated using a standard lamp while separately considering the window transmittance.

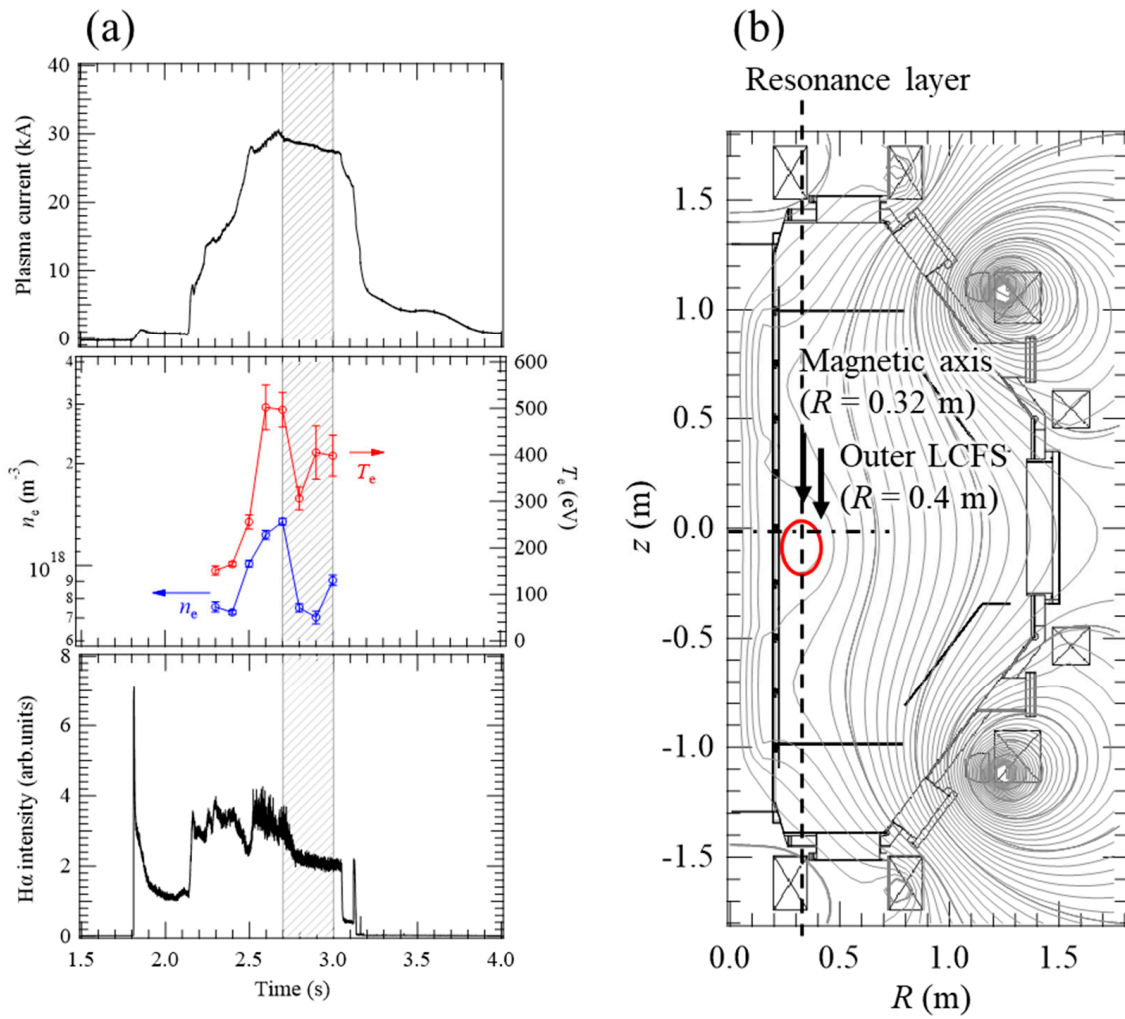


Figure 1. (a) Temporal evolutions of the plasma current, electron temperature, and density at the core ($R = 0.34$ m, $z = 0$ m) (#41176), and chord-integrated H α intensity (#41178). (b) Equilibrium magnetic flux surfaces in the time period $t = 2.7$ – 3.0 s denoted by the shaded area in (a). The last closed flux surface (LCFS) is shown by the red line.

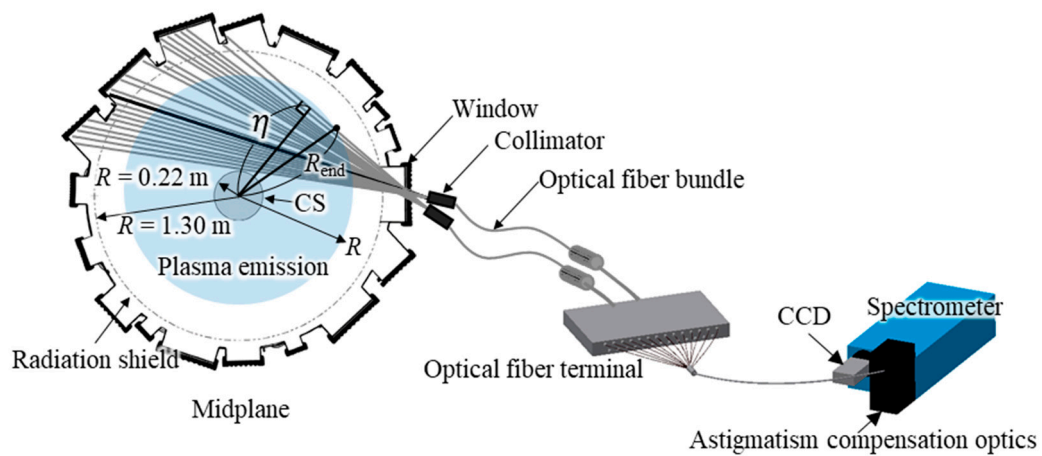


Figure 2. Schematic illustrations of the cross-section of the Q-shu University Experiment with Steady-State Spherical Tokamak (QUEST) midplane and the visible spectroscopic system.

3. Results

Figure 3a shows a H_δ spectrum measured on the viewing chord at $\eta = 0.51$ m, which is indicated by the bold line in Figure 2; this position corresponds to the outer scrape-off-layer (SOL). We evaluated the chord-integrated intensity I_A from the area of the spectrum. The evaluated I_A is marked in Figure 3b. The error bars consist of uncertainties in the sensitivity calibration coefficient and the zero level of the spectrum. Note that the pedestal of the OII emission line at 410.32 nm is superposed on that of H_δ , but its effect on I_A is small and we neglected it. Additionally, we omitted I_A obtained on the chord at $\eta = 0.84$ m owing to the large noise produced by the incidence of X-rays to the CCD.

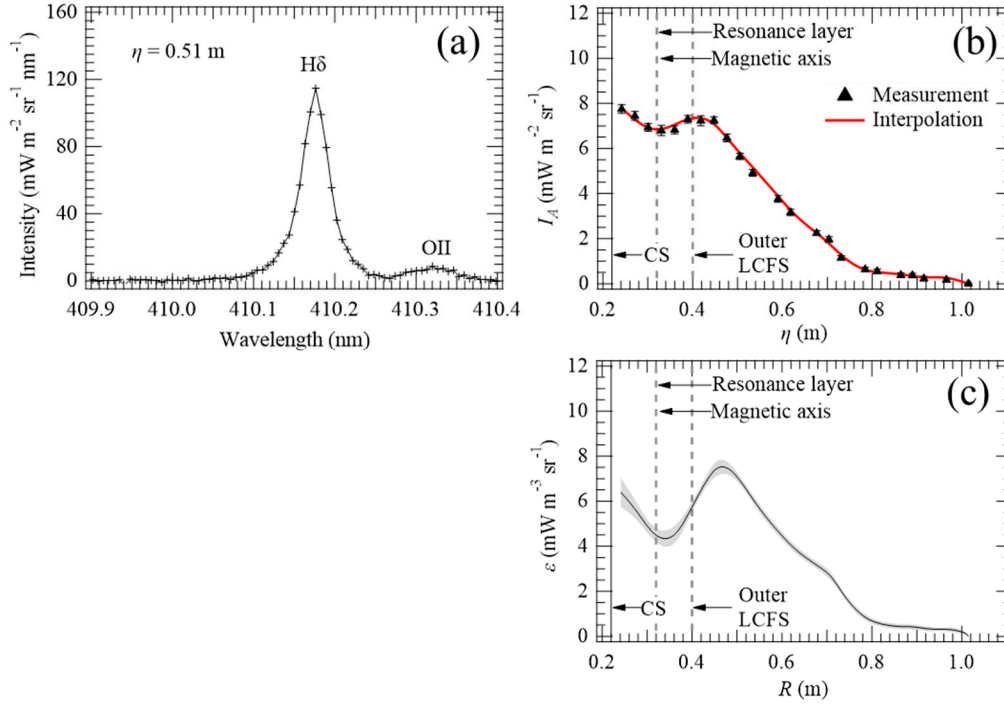


Figure 3. (a) H_δ spectrum measured on the viewing chord at $\eta = 0.51$ m (#41178). (b) Chord-integrated H_δ intensities and the interpolated curve. (c) Radial distribution of H_δ emissivity obtained using Abel inversion.

From the evaluated I_A , we calculated the radially resolved emissivity $\varepsilon(R)$ using Abel inversion assuming the toroidal symmetry of the emission. In a tokamak discharge with similar plasma parameters and wall conditions, the variation in H_α ($p = 2-3$) intensity in the toroidal direction was reported to be small except for an approximately 10 times local increase at the poloidal limiter [11]. Since the present discharge is limited by the center stack, the validity of the assumption of the toroidal symmetry could degrade near the center stack.

For the numerical calculation of the Abel inversion, the discrete data of I_A was interpolated with a smooth spline function in the range $\eta = 0.24-1.01$ m as shown by the red curve in Figure 3b. $\varepsilon(R)$ was then calculated as follows:

$$\varepsilon(R) = -\frac{1}{\pi} \int_R^{R_{\text{end}}} \frac{1}{\sqrt{\eta^2 - R^2}} \frac{dI_A(\eta)}{d\eta} d\eta, \quad (1)$$

where R_{end} is the outermost radius of H_δ emission, which we determined to be 1.01 m because I_A obtained on viewing chords at $\eta \geq 1.01$ m was less than the noise level. The calculated $\varepsilon(R)$ is shown in Figure 3c. We evaluated the error bar by the procedure described in [12] using 500 pairs of data. A small peak was found in $\varepsilon(R)$ around $R = 0.7$ m owing to an increase in I_A at $\eta = 0.71$ m. We confirmed the reproducibility of this tendency in identical discharges, but we have not identified its origin.

The hydrogen atom density was calculated from $\varepsilon(R)$ by collisional-radiative (CR) model analysis [13]. The atom density in an excited state p , $n_{H,p}(R)$, is expressed from the equation of continuity and the quasi steady-state approximation as follows:

$$n_{H,p}(R) = r_{0p}(R; T_e, n_e) n_{H^+}(R) n_e(R) + r_{1p}(R; T_e, n_e) n_H(R) n_e(R) + r_{2p}(R; T_e, n_e) n_{H_2}(R) n_e(R), \quad (2)$$

where n_{H^+} , n_H , and n_{H_2} are the ground-state hydrogen ion, atom, and molecule densities, respectively. r_{0p} , r_{1p} , and r_{2p} are called population coefficients whose values are calculated with a CR model code [13] as a function of T_e and n_e .

Figure 4 shows the calculated population coefficients for $p = 6$, where the green, red, and blue lines represent r_{06} , r_{16} , and r_{26} , and the solid, dashed, and dash-dotted lines are those at $n_e = 10^{16}$, 10^{17} , and 10^{18} m^{-3} , respectively. T_e and n_e of the present plasma are in the ranges of $10 \leq T_e \leq 400 \text{ eV}$ and $10^{16} \leq n_e \leq 10^{18} \text{ m}^{-3}$, respectively (see Figure 5a), and the former is denoted by the shaded area in Figure 4. Considering the relative magnitudes of the population coefficients and the approximated charge neutrality condition $n_{H^+} \cong n_e$, we can neglect the first term of Equation (2). We can also neglect the third term by assuming that $n_{H_2} < n_H$, which is reasonable except for near the wall. Equation (2) is then approximated as follows:

$$n_{H,6}(R) \cong r_{16}(R; T_e, n_e) n_H(R) n_e(R). \quad (3)$$

The excited hydrogen atom density $n_{H,6}(R)$ is obtained from $\varepsilon(R)$ using the following:

$$\varepsilon(R) = \frac{h\nu}{4\pi} n_{H,6}(R) A, \quad (4)$$

where h is the Planck constant and ν and A are the frequency and spontaneous emission coefficient of the H_δ transition, respectively. Then, $n_H(R)$ is obtained from Equations (3) and (4) as follows:

$$n_H(R) = \frac{4\pi}{h\nu A r_{16}(R; T_e, n_e) n_e(R)} \varepsilon(R). \quad (5)$$

We interpolated T_e and n_e measured by Thomson scattering [9] in the same way as I_A as shown in Figure 5a. In addition, the data was linearly extrapolated on the inboard side ($R = 0.28\text{--}0.34 \text{ m}$) to evaluate n_H around the resonance layer. The extrapolated curves are shown by dashed lines.

$n_H(R)$ evaluated with the above procedures is shown in Figure 5b. The density is in the range of $10^{15}\text{--}10^{16} \text{ m}^{-3}$ and monotonically decreases toward the ECH resonance layer. The increase around $R = 0.65 \text{ m}$ is physically implausible and may have been caused by an error in $\varepsilon(R)$. The evaluated density is less than the hydrogen molecule density of approximately 10^{17} m^{-3} at the vacuum chamber wall ($R = 1.3 \text{ m}$) obtained from the pressure measured by a fast ionization gauge assuming a temperature of 300 K.

The accuracy of the CR model analysis can be affected by the opacity of Lyman series emission lines ($p = 1\text{--}q$), where q is the upper-state principal quantum number [14]. When the opacity is significant, the reabsorption of Lyman series emission lines increases the excited hydrogen atom density, and ignoring the effect results in the overestimation of $n_H(R)$. Since the present CR model analysis is mainly affected by the L_ϵ line ($p = 1\text{--}6$) and the secondary effect, namely, the increase in $n_{H,6}(R)$ owing to the absorption of the other Lyman series emission lines, is small [14,15], we evaluated the effect of the opacity by calculating the optical depth of the L_ϵ line at its line center [16] under the assumption of a uniform plasma as follows:

$$\tau = \frac{e^2}{4m_e\epsilon_0} \sqrt{\frac{m_H}{2\pi k_B T_H}} \frac{f_{16}}{\nu_{16}} n_H L, \quad (6)$$

where e is the elementary charge, ε_0 is the vacuum permittivity, k_B is the Boltzmann constant, m_e is the electron mass, m_H is the hydrogen atom mass, f_{16} ($=7.8035 \times 10^{-3}$) and ν_{16} ($=3.1967 \times 10^{15}$ Hz) are the absorption oscillator strength and transition frequency, respectively, n_H is the density of ground-state atoms, and L is the absorption length. We assumed an identical temperature T_H for the excited and ground-state atoms. Assuming $T_H = 300$ K, $n_H = 1 \times 10^{16} \text{ m}^{-3}$, and $L = 2$ m gives the upper limit of the optical depth τ as 1.5×10^{-2} . The reabsorption with an optical depth of this magnitude is negligible in the CR model analysis.

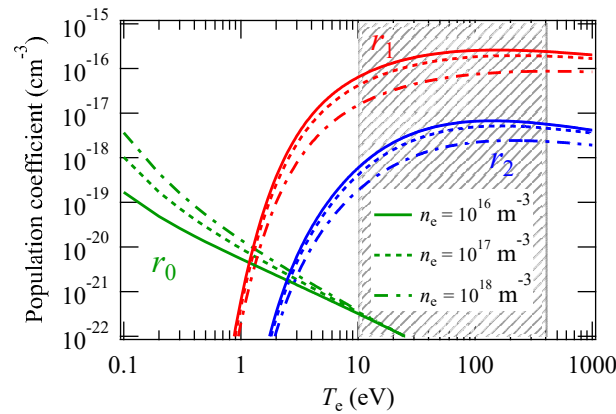


Figure 4. Population coefficients for $p = 6$. The green, red, and blue lines represent r_{06} , r_{16} , and r_{26} , respectively. The solid, dashed, and dash-dotted lines represent those at $n_e = 10^{16}$, 10^{17} , and 10^{18} m^{-3} , respectively.

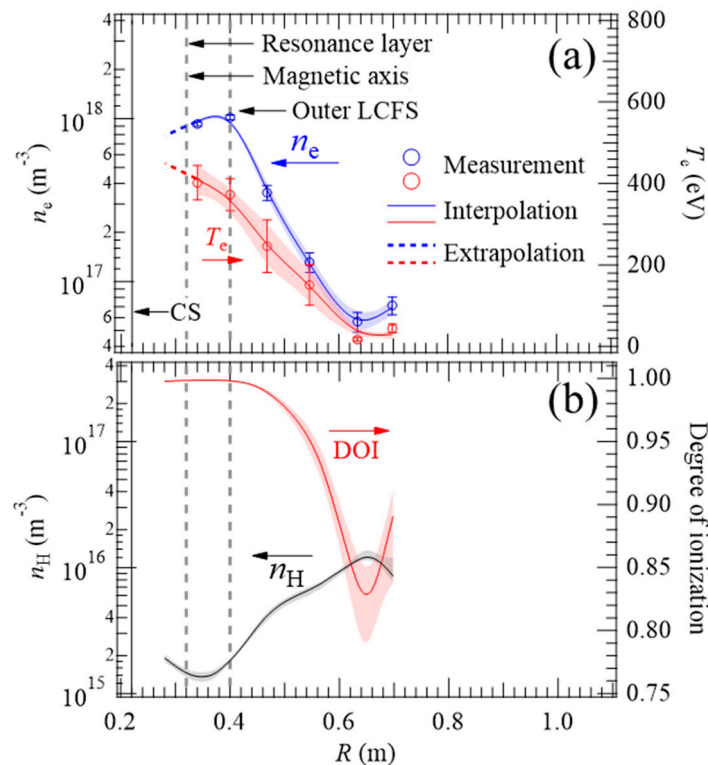


Figure 5. (a) T_e and n_e measured by Thomson scattering and their interpolated and extrapolated curves. (b) Evaluated n_H and the degree of ionization (DOI).

Finally, as a measure of the effect of atoms on the plasma, we evaluated the degree of ionization (DOI). The DOI is defined as $n_{H^+} / (n_{H^+} + n_H + n_{H_2})$ and we approximated it to $n_e / (n_e + n_H)$ on the basis of the above-mentioned assumptions, where we used the interpolated curve of n_e in

Figure 5a. The evaluated DOI shown in Figure 5b reached nearly unity over the entire core region, suggesting that the effect of atoms on the core plasma is small. The DOI, however, decreased in the SOL region and this could induce the momentum loss of the ions trapped in orbits that intersect the LCFS.

4. Conclusions

In this study, in order to evaluate the ion momentum loss and transport through the charge-exchange reactions in a QUEST plasma sustained only with 28 GHz ECH, we measured the radial distribution of the hydrogen atom density. The obtained density was of the order of 10^{15} – 10^{16} m^{−3}, and considering the fact that it is less than the hydrogen molecule density evaluated at the vacuum chamber wall and the observed tendency of a monotonic decrease toward the ECH resonance layer, the result is plausible. However, the effect of the violation of the assumed toroidally symmetric emission should be addressed to further improve the reliability of the result. The DOI evaluated using the atom density and n_e measured by Thomson scattering suggested that the effect of atoms is small in the core region.

Author Contributions: Conceptualization, T.S.; methodology, S.M., T.S., S.K., M.H. (Masahiro Hasuo), and K.S.; investigation, S.M., T.S., K.H., N.Y., A.K. and M.H. (Masahiro Hasuo); QUEST operation, K.H., H.I., T.O., T.I., K.N., R.I., Y.N., M.H. (Makoto Hasegawa), K.K., A.H., T.N. and S.S.; Thomson scattering measurements, A.E., Y.O., Y.P. and K.M.; writing—original draft preparation, S.M.; writing—review and editing, T.S.; funding acquisition, T.S. All authors have read and agreed to the published version of the manuscript.

Funding: This research was funded by JSPS KAKENHI (18K03576), bilateral (NIFS16KUTR114, NIFS19KUTR140), and LHD project research (NIFS16KOAP031) collaboration programs of the National Institute for Fusion Science, and the collaborative research program of the Research Institute for Applied Mechanics, Kyushu University (30FP-38).

Conflicts of Interest: The authors declare no conflict of interest.

References

1. Hanada, K.; Yoshida, N.; Hasegawa, M.; Hatayama, A.; Okamoto, K.; Takagi, I.; Hirata, T.; Oya, Y.; Miyamoto, M.; Oya, M.; et al. Particle balance investigation with the combination of the hydrogen barrier model and rate equations of hydrogen state in long duration discharges on an all-metal plasma facing wall in QUEST. *Nucl. Fusion* **2019**, *59*, 076007. [[CrossRef](#)]
2. Idei, H.; Kariya, T.; Imai, T.; Mishra, K.; Onchi, T.; Watanabe, O.; Zushi, H.; Hanada, K.; Qian, J.; Ejiri, A.; et al. Fully non-inductive second harmonic electron cyclotron plasma ramp-up in the QUEST spherical tokamak. *Nucl. Fusion* **2017**, *57*, 126045. [[CrossRef](#)]
3. Kuroda, K.; Raman, R.; Hanada, K.; Hasegawa, M.; Onchi, T.; Ono, M.; Nelson, B.A.; Jarboe, T.R.; Nagata, M.; Mitarai, O.; et al. Initial results from solenoid-free plasma start-up using transient CHI on QUEST. *Plasma Phys. Control. Fusion* **2018**, *60*, 115001. [[CrossRef](#)]
4. Maekawa, T.; Yoshinaga, T.; Uchida, M.; Watanabe, F.; Tanaka, H. Open field equilibrium current and cross-field passing electrons as an initiator of a closed flux surface in EC-heated toroidal plasmas. *Nucl. Fusion* **2012**, *52*, 083008. [[CrossRef](#)]
5. Yoneda, N.; Shikama, T.; Zushi, H.; Hanada, K.; Fujikawa, A.; Onchi, T.; Kuroda, K.; Nii, K.; Hasuo, M.; Hasegawa, M.; et al. Spectroscopic measurements of impurity ion toroidal and poloidal flow velocities and their dependence on vertical magnetic field in QUEST toroidal ECR plasmas. *Plasma Fusion Res.* **2018**, *13*, 3402087. [[CrossRef](#)]
6. Yoshinaga, T.; Uchida, M.; Tanaka, H.; Maekawa, T. Spontaneous formation of closed-field torus equilibrium via current jump observed in an electron-cyclotron-heated plasma. *Phys. Rev. Lett.* **2006**, *96*, 125005. [[CrossRef](#)] [[PubMed](#)]
7. Yoneda, N.; Shikama, T.; Hanada, K.; Mori, S.; Onchi, T.; Kuroda, K.; Hasuo, M.; Idei, H.; Nakamura, K.; Nagashima, Y.; et al. Toroidal flow measurements of impurity ions in QUEST ECH plasmas using multiple viewing chords emission spectroscopy. *Nucl. Mater. Energy* **2020**, submitted.
8. Versloot, T.W.; de Vries, P.C.; Giroud, C.; Brix, M.; von Hellermann, M.G.; Lomas, P.J.; Moulton, D.; O'Mullane, M.; Nunes, I.M.; Salmi, A.; et al. Momentum losses by charge exchange with neutral particles in H-mode discharges at JET. *Plasma Phys. Control. Fusion* **2011**, *53*, 065017. [[CrossRef](#)]

9. Yamaguchi, T.; Ejiri, A.; Hiratsuka, J.; Hasegawa, M.; Nagashima, Y.; Narihara, K.; Takase, Y.; Zushi, H.; The QUEST Group. Electron Temperature Measurement on QUEST Spherical Tokamak by Thomson Scattering System. *Plasma Fusion Res.* **2015**, *10*, 1202082. [[CrossRef](#)]
10. Yoshinaga, T.; Uchida, M.; Tanaka, H.; Maekawa, T. A current profile model for magnetic analysis of the start-up phase of toroidal plasmas driven by electron cyclotron heating and current drive. *Nucl. Fusion* **2007**, *47*, 210. [[CrossRef](#)]
11. Zushi, H.; Nakamura, K.; Hanada, K.; Sato, K.N.; Sakamoto, M.; Idei, H.; Hasegawa, M.; Iyomasa, A.; Kawasaki, S.; Nakashima, H.; et al. Steady-state tokamak operation, ITB transition and sustainment and ECCD experiments in TRIAM-1M. *Nucl. Fusion* **2005**, *45*, S142. [[CrossRef](#)]
12. Ueda, A.; Shikama, T.; Teramoto, T.; Higashi, T.; Iida, Y.; Hasuo, M. Spectroscopic measurement of the degree of ionization in a helium electron cyclotron discharge in a simple cusp field. *Appl. Phys. Lett.* **2017**, *111*, 074101. [[CrossRef](#)]
13. Sawada, K.; Fujimoto, T. Effective ionization and dissociation rate coefficients of molecular hydrogen in plasma. *J. Appl. Phys.* **1995**, *78*, 2913. [[CrossRef](#)]
14. Sawada, K.; Goto, M.; Ezumi, N. Spectroscopic Diagnostic of Helium-Hydrogen RF Plasma under the Influence of Radiation Trapping. *Plasma Fusion Res.* **2011**, *6*, 1401010. [[CrossRef](#)]
15. Ueda, A.; Shikama, T.; Teramoto, T.; Higashi, T.; Iida, Y.; Hasuo, M. Helium atom line-intensity ratios as an integrated diagnostic tool for low-pressure and low-density plasmas. *Phys. Plasmas* **2018**, *25*, 054508. [[CrossRef](#)]
16. Shikama, T.; Ogane, S.; Iida, Y.; Hasuo, M. Measurement of the helium 2^3S metastable atom density by observation of the change in the 2^3S – 2^3P emission line shape due to radiation reabsorption. *J. Phys. D Appl. Phys.* **2016**, *49*, 025206. [[CrossRef](#)]



© 2020 by the authors. Licensee MDPI, Basel, Switzerland. This article is an open access article distributed under the terms and conditions of the Creative Commons Attribution (CC BY) license (<http://creativecommons.org/licenses/by/4.0/>).